

## Normalized Free Energy and Normalized Entropy Applied to Some Lambda ( $\lambda$ ) Transitions

Peter Love<sup>1,2</sup>

---

The  $\lambda$ -anomaly occurs for a system that can undergo a boson – fermion thermodynamic equilibrium. It is shown that a  $\lambda$ -transition figure can be interpreted in terms of the normalized Gibbs–Helmholtz equation, the Maxwell–Boltzmann energy distribution function, and properties of the statistics of the relevant species. There are three variations of a “ $\lambda$ -transition” curve. These are: (A) the classical  $\lambda$  curve, (B) a saw-tooth line shape that is characteristic of the Bardeen–Cooper–Schrieffer theory of superconductivity, and (C) a single line  $\delta$  type figure. The low temperature He-4 transition, and Type II superconductor transitions are typical of the line shape A. Type I superconductors typically have type B line shapes. The line shapes for variations A and C result from classical thermodynamic equilibria. The type B line shape occurs in systems that do not have a classical thermodynamic equilibrium at the superconducting transition. Analysis of type B line shapes provides interesting concepts and data for some low- and high-temperature superconductors. Several applications and physical property consequences of these line shapes are discussed.

---

**KEY WORDS:** heat capacity; lambda anomaly; magnetic heat capacity; superconductivity; superfluidity.

### 1. INTRODUCTION

A lambda,  $\lambda$ , anomaly occurs in a heat capacity at constant pressure,  $c_p$ , versus temperature curve for a second-order phase transition. There is a  $c_p$  maximum at the equilibrium temperature,  $T_\lambda$ . The heat capacity at, and near,  $T_\lambda$  has the shape of the lower case Greek letter,  $\lambda$ . Thus, the terms,

---

<sup>1</sup> Department of Chemistry, University of Connecticut at Stamford, 1 University Place, Stamford, Connecticut 06901-2315, U.S.A.

<sup>2</sup> To whom correspondence should be addressed. E-mail: peter.love@uconn.edu

“lambda-transition,” or “lambda-function” are commonly used. It is the purpose here to logically explain the line shape of the  $\lambda$ -function in simple conceptual terms. From this, one can understand the different types of  $\lambda$ -functions, and the apparently anomalous occurrence of a metallic phase between some observed insulator-to-superconductor transitions.

An example of the  $\lambda$ -function is the “anomaly” that occurs in the often discussed transition of  $^4\text{He}$  [1]. This occurs for the equilibrium between helium II (superfluid phase) and helium I (normal fluid phase). This can be written as



The  $\lambda$ -function occurs in diverse chemical and physical systems at temperatures from about 1 to 1000 K. This shows that the anomaly is not a function of any given system. It is the result of thermodynamic constraints on the energy and the statistics of a system.

## 2. THERMODYNAMIC CRITERIA FOR SUPERFLUIDITY AND SUPERCONDUCTIVITY

The well known Gibbs–Helmholtz equation for an adiabatic isobaric system is

$$\Delta H = \Delta G + T \Delta S. \quad (2)$$

Dividing Eq. (2) by  $\Delta H$  one obtains Eq. (3) in terms of the normalized free energy,  $\Delta G_n$ , and normalized entropy,  $\Delta S_n$  [2]. This yields

$$\Delta G_n + T \Delta S_n = 1. \quad (3)$$

In Eq. (3),

$$\Delta G_n = \Delta G / \Delta H, \quad (4)$$

$$\Delta S_n = \Delta S / \Delta H, \quad (5)$$

and  $T$  is the absolute temperature.

The enthalpy change,  $\Delta H$ , is the total energy change in such a system. The Gibbs free energy,  $\Delta G$ , can be defined as the available energy change in a system that can be converted to perform, or achieve, a specific goal, or task. Thus,  $\Delta G$  represents the available energy change capable of performing “useful” work. Then  $T \Delta S$  is the change in energy that is not available to perform the specific goal, or task. To rephrase this,  $T \Delta S$

represents the energy change that is not capable of performing, or achieving, “useful” work.

Superfluidity involves the dynamics, and/or energetics of the state, or motion, of atomic or molecular systems. Superconductivity involves comparable properties of conduction electrons in a system. The  $\lambda$ -transition line shapes of  $^4\text{He}$ , and some high-temperature superconductors, e.g.,  $\text{Bi}_2\text{Sr}_2\text{Ca}_2\text{Cu}_3\text{O}_x$ , are essentially superimposable with graphical scaling [3]. One expects that the same thermodynamic processes and equations are applicable for the  $\lambda$ -functions of these diverse systems.

Conceptually one can characterize superfluidity and superconductivity in terms of the normalized parameters,  $\Delta G_n$  and  $\Delta S_n$ . The two “super” states have similar properties.

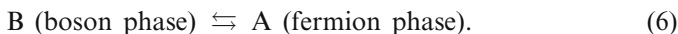
(a) Normalized entropy,  $\Delta S_n \rightarrow 0$ , i.e.,  $\Delta S_n$  becomes minimized, or negligibly small.

(b) In terms of Eq. (3), property a implies that the normalized free energy,  $\Delta G_n \rightarrow 1$ .

From the definition of  $\Delta G_n$  as shown by Eq. (4) it follows that when,  $\Delta G_n \rightarrow 1$ , then  $\Delta G \rightarrow \Delta H$ . Thus, in principle, when  $\Delta S_n \rightarrow 0$ , the total enthalpy change of the phase is convertible to purely Gibbs free energy,  $\Delta G$ . Superfluidity and superconductivity are physical states in which normalized Gibbs free energy is maximized, and normalized entropy is minimized. The value of  $T\Delta S_n$  is sufficiently small that it cannot act as an effective dissipative energy sink for the species in this state.

### 3. NATURE OF A $\lambda$ -TRANSITION

A  $\lambda$ -transition anomaly of a  $c_p$  versus temperature curve is a graphical representation of the dynamics of the processes that occur at, and near, the temperature of maximum  $c_p$ ,  $T_\lambda$ . Consider a general second-order phase transition for species A (normal fermion phase) and species B (“super” or boson phase) comparable to that for  $^4\text{He}$  as an example. This is shown in Fig. 1. Equation (1) can be rewritten as



One can postulate a facile dynamic equilibrium,  $\text{B} \rightleftharpoons \text{A}$ , that occurs at  $T_\lambda$ . From the Gibbs–Helmholtz equation at equilibrium, the free energy is minimized, i.e.,  $\Delta G = 0$ . Therefore,  $\Delta G_n = 0$ . Then from Eq. (3),  $T\Delta S_n \rightarrow 1$ . At  $T_\lambda$ ,  $\Delta S_n$  is a maximum. One can write for the entropy change,  $\Delta S$ , of a reaction

$$\Delta S = c_p \ln T. \quad (7)$$

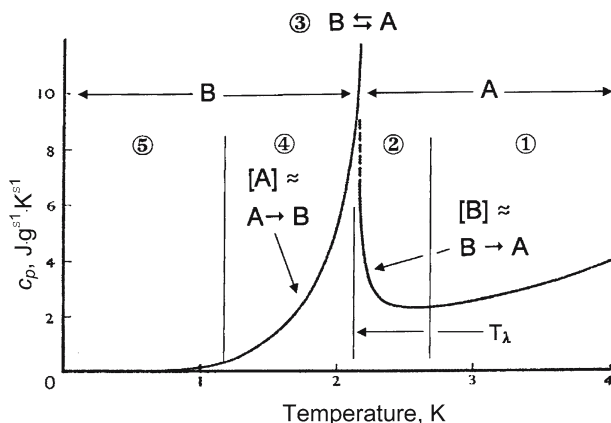


**Fig. 1.** Regions of a Type A  $\lambda$ -function in the heat capacity versus temperature curve for a second-order phase transition.

For the equilibrium reaction, Eq. (6),  $\Delta H$  is a small finite quantity. At  $T_\lambda$ ,  $\Delta H = T\Delta S$ . Since  $\Delta S$  is a maximum at  $T_\lambda$  then according to Eq. (7)  $c_p$  also has a finite maximum value. By one definition,  $c_p = \text{energy}_{\text{input}} \times \text{mass}^{-1} \times \text{temperature}^{-1}$ . Then at  $T_\lambda$  the system is a relatively large energy sink. The energy absorbed goes into the lowest entropy mode(s) available. In this case it results in enhancement of the equilibrium between species B and A.

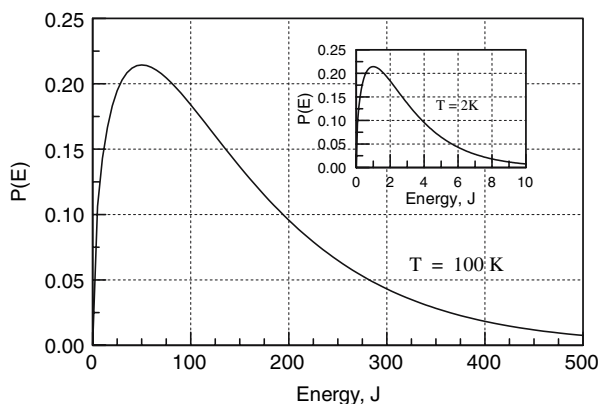
A  $\lambda$ -transition curve can be considered to consist of five general regions. In the order of decreasing temperature these are: (1) species A, (2) species A and metastable B, [B], in species A, (3) species B in equilibrium with species A, (4) species B and metastable A, [A], in species B, and (5) species B. These are given in Table I and illustrated in Fig. 1. The temperature ranges of regions shown in Table I correspond to,  $T_\lambda = 2.17$  K, for the  $\lambda$ -transition in  $^4\text{He}$ . Regions 2 and 4 are not what one might expect at first thought. They are the consequences of the equilibrium,  $B \rightleftharpoons A$ , that occurs at  $T_\lambda$ .

Numerically when,  $\Delta G_n = 0$ , the temperature has a singular value,  $T_\lambda$ . However, the energy values of B and A are not singular at a given temperature. Each species has a range of energies nominally given by the Maxwell-Boltzmann distribution function,  $P(E)$ . One version of this function is

$$P(E) = \frac{2}{\pi^{1/2}(kT)^{3/2}} E^{1/2} e^{-(E/kT)} \Delta E \quad (8)$$

**Table I.** Possible Assignments of Regions of a Type A  $\lambda$ -Transition Curve

Region	Temperature Range (K)	Species in Region
1	$T \gtrsim 2.7$	A
2	$T_\lambda - \sim 2.7$	$B \rightarrow A$ ; $\Delta H = (+)$ , and A
3	$T_\lambda$	$A \rightleftharpoons B$ ; $\Delta G = 0$
4	$\sim 1.2 - T_\lambda$	$A \rightarrow B$ ; $\Delta H = (-)$ , and B
5	$\lesssim 1.2$	B

**Fig. 2.** Probability,  $P(E)$ , that a species has kinetic energy between  $E$  and  $\Delta E$  at 100 K, and at 2 K (insert).

This distribution function is shown in Fig. 2 for temperatures of 100 K, and 2 K in the inset figure. As shown in Fig. 2, the highest energies of a species are about ten times the value of the maximum, or average, energy of the species. It is the higher, or highest, energy A species, [A], that exist in Region 4.

The highest energy A species can exist at temperatures below  $T_\lambda$ . These are indicated as the metastable state, [A]. The lowest energy B species result in the existence of B above  $T_\lambda$ , and are indicated as [B]. Thus, in the asymptotic regions about  $T_\lambda$ , the highest energy [A] species can exist at temperatures below  $T_\lambda$ , and the lowest energy [B] species can exist at temperatures above  $T_\lambda$ .

It is generally observed that a  $\lambda$ -function is skewed to the left. That is, the area under the low-temperature wing below  $T_\lambda$  is greater than the area of the high-temperature wing above  $T_\lambda$ . This follows by considering the entropy resulting from the quantum state multiplicity,  $Q$ , of the fermion species, A ( $Q > 1$ ), and of the boson species, B ( $Q = 1$ ). The Boltzmann

equation for entropy is,  $S = k_B \ln Q$ . Here  $k_B$  is the Boltzmann constant. Then, the entropy change for the change in multiplicity is  $\Delta S_Q$  [4].

$$\Delta S_Q = S_A - S_B = k_B \ln Q_A - k_B \ln Q_B = k_B \ln(Q_A/Q_B) \quad (9)$$

The value of  $c_p$  at  $T_\lambda$  for  ${}^4\text{He}$  can be estimated from Fig. 1. From Eqs. (7) and (9), one obtains  $(Q_A/Q_B) \approx 10$ . Since,  $Q_A/Q_B > 1$ , the reaction, Eq. (1), is spontaneous to the right since,  $\Delta S = (+)$ . Then at equilibrium, i.e., at  $T_\lambda$ , the concentration of A is greater than the concentration of B. Therefore, for the metastable species in the asymptotic regions about  $T_\lambda$ ,  $[A] > [B]$ . This is in agreement with the observation that the  $\lambda$ -function is skewed to the left.

Also, it is known that when other factors, e.g., density of states and temperature interval, are considered constant, the population of boson states is skewed toward lower-lying energies, and the population of fermions is skewed toward higher-lying energies [5]. Such population distributions also lead to the conclusion that at  $T_\lambda$  the concentration of A is greater than the concentration of B.

For  ${}^4\text{He}$  Wilks [6] gives equations for the specific heat wings in the small temperature interval about  $T_\lambda$ , and shows that they are logarithmically asymptotic to  $T_\lambda$ . By differentiating those asymptotic equations for  $c_p$  with respect to  $T - T_\lambda$ , and rearranging terms, one finds that in these regions,  $c_p \approx |T - T_\lambda|^{-1}$ . The logarithmic temperature dependence of the curve in Region 2 implies that the species concentration is proportional to  $|T - T_\lambda|^{-1}$ . Such a property at temperatures above  $T_\lambda$  can only be ascribed to B existing in, and being converted to, A. As previously stated this is indicated as [B]. Likewise, in Region 4 which is below  $T_\lambda$ , the logarithmic curve represents the concentration of A in B, i.e., [A].

In an excellent and detailed study of the high-temperature superconductor,  $\text{Bi}_2\text{Sr}_2\text{Ca}_2\text{Cu}_3\text{O}_x$ , Schnelle et al. [7] show that for the  $\lambda$ -function the wings, or shoulders, about  $T_\lambda$  are logarithmic. Schnelle et al. [7] show clearly that the low-temperature wing has a larger area, or extends over a wider temperature range, than the high-temperature wing. This is as expected from the above discussion.

The conductivity data for  $\text{Bi}_2\text{Sr}_2\text{Ca}_2\text{Cu}_3\text{O}_x$  supports these assignments. Schnelle et al. [7] describe "superconducting fluctuations" in a range on the order of  $\pm 10$  K about  $T_c$ . The logarithmically decreasing resistivity starting about 10 K above  $T_c$  can be considered as experimental verification of the existence of [B] in A above  $T_\lambda$ . This corresponds to Region 2 in Fig. 2. The "superconducting fluctuations" referred to by Schnelle et al. [7] correspond to this [B] in A. In their discussion these authors state that, "... some entropy is shifted from below to above

$T_c$  by the fluctuations.” They explain this in terms of Ginzburg–Landau theory. A simpler explanation is that given above in terms of the Maxwell–Boltzmann energy distribution. These authors describe “critical behavior within  $-17$  and  $+8.5$  K of  $T_c$ ” [7]. The first larger number,  $-17$  K, is indicative of [A] in B, and  $8.5$  K corresponds to [B] in A.

The  $\lambda$ -functions that occur in high-temperature ( $\sim 1000$  K) magnetic heat-capacity data for elements such as cobalt and iron show the same results. The logarithmic form of the asymptotic wings about  $T_\lambda$  is clearly shown in figures given by de Fontaine et al. [8]. Likewise, the characteristic larger area of the low-temperature wing relative to the high-temperature wing is clearly shown [8]. Thus, by thermodynamic reasoning, the logarithmic form of the  $\lambda$ -function wings, experimental heat-capacity data, and the electrical conductivity near a superconducting transition support the same conclusion. In the asymptotic regions about  $T_\lambda$ , the low-temperature wing of a  $\lambda$ -function results from [A] in B below  $T_\lambda$ , and the high-temperature wing is due to [B] in A above  $T_\lambda$ .

#### 4. INSULATOR–SUPERCONDUCTOR TRANSITIONS

In an interesting article Phillips and Dalidovich [9] note the unexpected occurrence of a metallic phase between some low-dimensional insulator–superconductor transition systems. Insulator–superconductor transitions are analogous to normal liquid–superfluid transitions that are discussed in Section 3. These authors cite conductivity experiments on homogeneously disordered films of elements such as Ga, Al, Pb, and In.

For an insulator–superconductor equilibrium transition at  $T_\lambda$ ,  $\Delta G_n = 0$ . Therefore,  $T_\lambda \Delta S_n \rightarrow 1$ . The entropy is a maximum at the transition temperature. Thus, for the entropy function one goes from an insulator A (low entropy)  $\rightarrow$  intermediate equilibrium species (very high entropy)  $\rightarrow$  superconductor B (very low entropy). The very high entropy equilibrium species corresponds to major electron delocalization. Also, at  $T_\lambda$  there is a significant amount of the insulator phase that corresponds to A as discussed in Section 3. Therefore, the intermediate phase will be resistive, i.e., metallic. The existence of a metallic phase between insulator and superconductor phases is expected to depend on whether a *thermodynamic* equilibrium exists between these two phases, A and B. If the transition, insulator  $\rightarrow$  superconductor, is a thermodynamic equilibrium, then the high entropy intermediate metallic phase necessarily exists.

Phillips and Dalidovich [9] emphasize that it is the “phase locking” of Cooper pair bosons into a single quantum state that is responsible for superconductivity. They state that it is the breaking of phase coherence of boson states that result in intermediate metallic behavior. The “breaking

of phase coherence of boson states” in thermodynamic terms can be interpreted as “a large increase in entropy” for the intermediate metallic state. One can argue that the necessary dramatic entropy increase at, or near, the equilibrium transition temperature is responsible for phase coherence breaking, and the existence of an intermediate metallic phase. The entropy of conduction electrons in a metallic state is much higher than that of the corresponding superconductor, or that of the corresponding insulator phase.

## 5. DISCUSSION

### 5.1. Types of $\lambda$ -Functions

There are basically three types of “ $\lambda$ -anomaly” figures that occur in heat capacity versus temperature curves. These are: (A) the classical  $\lambda$ -anomaly figure that has high- and low-temperature wings, or shoulders, about  $T_\lambda$ , (B) the discontinuous Bardeen–Cooper–Schrieffer (BCS) type that has a low-temperature wing, but no high-temperature wing, and (C) the  $\delta$ -type anomaly that consists of a singular  $\delta$ -type function without any wings. This can be termed as a “singular”  $\lambda$ -function.

The type of  $\lambda$ -anomaly that occurs is a function of the value of the Fermi energy,  $E_F$ , of species A relative to the value of the ambient energy at  $T_\lambda$ . When  $E_F$  is sufficiently low, a type A  $\lambda$ -function can occur. When  $E_F$  is sufficiently high, a type B  $\lambda$ -function will result.

#### 5.1.1. Type A $\lambda$ -Functions

This type of  $\lambda$ -anomaly results from a system that has a thermodynamic equilibrium between B and A at  $T_\lambda$ . This is shown in Fig. 1. The species B and A can coexist in the same phase. This type is discussed in Section 3. It corresponds to “Type II superconductors” as is designated in the solid-state-physics literature. This type also occurs in high-temperature magnetic spin transitions for iron ( $T_c = 1039$  K), cobalt ( $T_c = 1377$  K), and nickel ( $T_c = 631$  K) [8]. In solid-state physics, the transition temperature is designated as  $T_c$ . From the results of Schnelle et al. [7], one can show that  $T_c \neq T_\lambda$ .

#### 5.1.2. Type B $\lambda$ -Functions

This type of anomaly has a saw-tooth line shape and a discontinuity at  $T_\lambda$ . An example is the heat-capacity curve for gallium that is shown in Fig. 3. This is a characteristic of “Type I superconductors.” Such an anomaly does *not* have a thermodynamic equilibrium between B and A at  $T_\lambda$ . It is true that transitions between B and A can occur with an appropriate



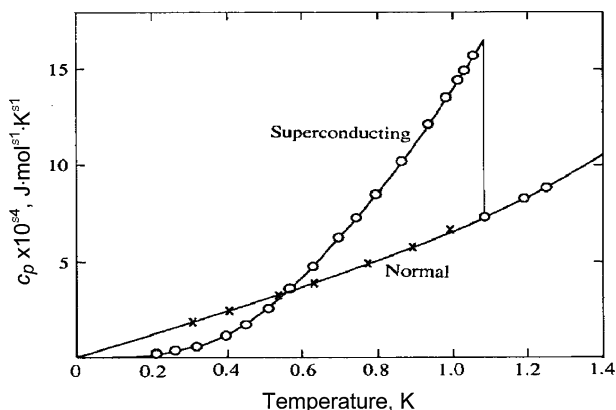


**Fig. 3.** Type B  $\lambda$ -function in the heat capacity versus temperature curve for gallium at  $T_c = 1.09$  K [13].

change in temperature. However, the two states are not in thermodynamic equilibrium. When one starts at  $T > T_\lambda$  on decreasing  $T$ ,  $c_p$  undergoes a discontinuous increase at  $T_\lambda$ . The discontinuity corresponds to the fermion  $\rightarrow$  boson transition. This discontinuity is common to both Type A and Type B  $\lambda$ -functions. On examining Fig. 1 carefully, one can see the discontinuity superimposed on the  $c_p$  maximum at  $T_\lambda$ .

In Fig. 3 the low-temperature wing just below  $T_c$  is an approximately linear decreasing function to the temperature where it intersects the  $c_p$  line of the normal state. It results from the presence of a metastable species in B. This is true for many low-temperature elemental superconductors with transition temperatures,  $T_c \lesssim 12$  K, and for the interesting higher-temperature  $\text{MgB}_2$  material with  $T_c = 39$  K [10]. It is understood that low-temperature BCS superconductors involve different superconductor formation mechanisms than those involved in high-temperature superconductors [3].

The  $c_p$  discontinuity for a Type B anomaly can be expected since the reaction,  $B \rightarrow A$ , for  $T \lesssim T_c$  is energetically blocked by the high value of the Fermi energy,  $E_F$ , of the normal A phase. The value of  $E_F$  of typical low-temperature superconducting elements is on the order of  $< 2\text{--}10$  eV [11]. The corresponding  $T_c$  values of such elements are on the order of  $< 1\text{--}10$  K [12]. As an example, for  $T_c = 5$  K, the value of the ambient energy,  $k_B T_c = \sim 10^{-4}$  eV. At this temperature,  $E_F \gtrsim 10^4 k_B T_c$ . Excitation of electrons into a conduction band normally occurs for energies  $\lesssim 4 k_B T_c$ . Therefore, at  $T_c$ , electron excitation for the reaction,  $B \rightarrow A$ , is blocked. The equilibrium,  $B \rightleftharpoons A$ , cannot occur. This is an example of the

proverbial Maxwell demons in action. This is in keeping with the principle of minimum entropy production.

The ambient energy that went into the equilibrium,  $B \rightleftharpoons A$ , for Type II superconductors must now go into another entropy mode for Type I materials. The most logical mode is an equilibrium phasing – dephasing of the Cooper pair boson quantum state below  $T_c$ . The approximately linear portion of the  $c_p$  versus  $T$  curve corresponds to Phillips and Dalidovich's [9] “phase locking” in the superconducting phase. It is described by the equation,

$$c_p = (\partial S / \partial T)_P T \approx (\Delta S / \Delta T)_P T. \quad (10)$$

Blakemore [13] states that below  $T_c$ ,  $c_p$  is demonstrably an exponential function. The simple incremental form of Eq. (10) yields for the  $\lambda$ -function of Ga [13],

$$c_p = 2.4 \times 10^{-4} T. \quad (11)$$

The increase in phase coherence with decreasing temperature along the linear section of the  $c_p$  curve should be observable by suitable dc Josephson-effect experiments.

By use of the procedure discussed in Section 3, Eqs. (7) and (9) yield at  $T_c$  for the  $\lambda$ -function of Ga [13],  $(Q_A/Q_B) = 1$ . This is true for Type I materials, such as Al [14], Ga [13], and MgB<sub>2</sub> [10]. If this result is valid, then an interesting conclusion can be made. It implies that at  $T_c$  when the transition discontinuity occurs, A has already decayed to a single quantum state. This result is in agreement with the assertion that at  $T_c$  the equilibrium,  $B \rightleftharpoons A$ , does not exist for Type I superconductors. The total entropy for the,  $A \rightarrow B$ , transition corresponds to the area of the saw-tooth triangular region in Fig. 3. This will be discussed elsewhere.

### 5.1.3. Type C $\lambda$ -Functions

Type C anomalies occur in systems where either A, or B, is stable. This corresponds to magnetic systems where the transition energy,  $\Delta H_\lambda$ , is large enough so that a facile equilibrium between A and B cannot occur at the ambient temperature,  $T_\lambda$ . These correspond to a  $c_p$  maximum at  $T_\lambda$  without any,  $B \rightleftharpoons A$ , equilibria. The singular  $\delta$ -type figures shown by de Fontaine et al. [8] for Cr and MnO are examples of Type C anomalies. The  $c_p$  anomaly for chromium at  $T_c = 311$  K is reproduced in Fig. 4.

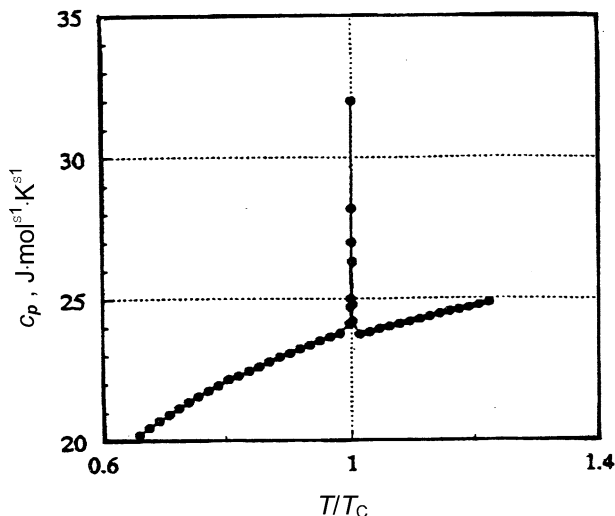


Fig. 4. Type C  $\lambda$ -function in the heat capacity versus temperature curve for chromium at  $T_c = 311$  K [8].

## 5.2. Relationship of Free Energy and Entropy

Callen [15] notes that in an equilibrium system the energy is minimized for a given value of total entropy. Equivalently for an equilibrium system, the entropy is maximized for a given value of total energy. It can also be stated that for an equilibrium system when the normalized free energy is minimized the normalized entropy is maximized. This is concisely expressed in Eq. (3). Thus, at equilibrium,  $\Delta G_n$  is zero and  $\Delta S_n$  is a maximum at  $T_\lambda$ . Likewise, when the normalized entropy is minimized, the normalized free energy is maximized. This occurs in the superfluid and superconductive states, where when  $\Delta S_n \rightarrow 0$ , then  $\Delta G_n \rightarrow 1$ .

Both Baierlien [16] and Stowe [17] note that for a boson species the chemical potential must be less than the energy of the lowest-lying state. Stowe notes that the Gibbs free energy is the same as the thermodynamic potential. Since  $\Delta G$  is the negative, the boson species, in principle, is capable of doing useful work. Thus, the negative chemical potential can be considered as the basis of persistent currents that are observed for superconductors.

## 6. CONCLUSION

The classical  $\lambda$ -transition anomaly that occurs in the heat capacity versus temperature curve for a second-order phase transition is one out of

three such line shapes that are observed experimentally. The classical line shape results from a thermodynamic equilibrium that exists between boson and fermion species at the transition temperature,  $T_\lambda$ , and in a narrow range of temperatures about  $T_\lambda$ . This can be used to explain the observed heat-capacity anomalies for the normal-to-superfluid  $^4\text{He}$  transition, those for Type II superconducting transitions, and those for high-temperature magnetic spin transitions. When the Fermi level of a normal state species is sufficiently high, a thermodynamic equilibrium is blocked. The entropy of the system is diverted into a phasing – dephasing mode that results in a saw-tooth line-shaped figure that is a characteristic of Type I superconductor transitions. Some magnetic spin-flip processes result in a singular  $\delta$  line shape. Thermodynamic considerations of a  $\lambda$ -transition can be used to explain the intermediate metallic state that occurs in some low-dimensional insulator-superconductor systems and the occurrence of the logarithmic decreasing resistivity of Type II superconductors just above  $T_c$ .

## REFERENCES

1. J. Wilks, *The Properties of Liquid and Solid Helium* (Clarendon Press, Oxford, 1967), p. 3.
2. P. Love, *Physical Chemistry Abstracts*, 224th ACS National Meeting (2002), p. 309.
3. A. S. Alexandrov and J. Ranninger, *Solid State Commun.* **81**:403 (1992).
4. R. Baierlein, *Thermal Physics* (Cambridge, Cambridge, 2001), pp. 33–37.
5. K. Stowe, *Introduction to Statistical Mechanics and Thermodynamics* (Wiley, New York, 1984), pp. 435–437.
6. J. Wilks, *The Properties of Liquid and Solid Helium* (Clarendon Press, Oxford, 1967), pp. 293–294.
7. W. Schnelle, E. Braun, H. Broicher, H. Weiss, H. Geus, S. Ruppel, M. Galffy, W. Braunsch, A. Waldorf, F. Seidler, and D. Wohlleben, *Physica C* **161**:123 (1989).
8. D. de Fontaine, S. G. Fries, G. Inden, P. Miodownik, R. Schmid-Fetzer, and S. L. Chen, *Calphad* **19**:499 (1995).
9. P. Phillips and D. Dalidovich, *Science* **302**:243 (2003).
10. F. Bouquet, R. A. Fisher, N. E. Phillips, D. G. Hinks, and J. D. Jorgensen, *Phys. Rev. Lett.* **87**:047001 (2001).
11. N. W. Ashcroft and N. D. Mermin, *Solid State Physics* (Saunders, Philadelphia, 1976), p. 38.
12. N. W. Ashcroft and N. D. Mermin, *Solid State Physics* (Saunders, Philadelphia, 1976), p. 729.
13. J. S. Blakemore, *Solid State Physics*, 2nd Ed. (Cambridge, Cambridge, 1985), pp. 270, 271.
14. N. W. Ashcroft and N. D. Mermin, *Solid State Physics* (Saunders, Philadelphia, 1976), p. 734.
15. H. B. Callen, *Thermodynamics* (Wiley, New York, 1962), p. 88.
16. R. Baierlein, *Thermal Physics* (Cambridge, Cambridge, 2001), pp. 200, 201.
17. K. Stowe, *Introduction to Statistical Mechanics and Thermodynamics* (Wiley, New York, 1984), p. 407.